Supplemental Materials

Molecular Biology of the Cell

Chehab et al.

Supplementary Information

Materials and methods

Antibodies

Antibodies directed against Munc13s were generated as rabbit polyclonal antibodies against isoform-specific protein fragments as described before (Varoqueaux *et al.*, 2005; Man *et al.*, 2015). Munc13-4 was detected in Western blots using a rabbit polyclonal antibody against human Munc13-4 (Shirakawa *et al.*, 2004); kindly provided by Hisanori Horiouchi, Tohoku University, Japan) or a commercial goat polyclonal antibody against human Munc13-4 (Imgenex/Novus Biologicals, NB100-1434). For loading controls, mouse anti-alpha-tubulin (Sigma-Aldrich, Catalog number), mouse anti-VCP (BD Biosciences, 612182), mouse anti-vimentin antibodies (Dianova, 07299) and mouse anti-calnexin (BD Transduction Laboratories, 610524) were employed. IRDye-coupled antibodies (LICOR) or HRP-coupled antibodies (Dako, Thermo Scientific) were used as secondary antibodies in Western blot analyses. Immunoprecipitations were carried out with rabbit polyclonal anti-Munc13-4 antibodies (Proteintech, 16905-1-AP), and for immunofluorescence we employed rabbit polyclonal anti-Munc13-4 antibodies from Santa Cruz Biotechnology (H-150, sc-50465) and anti-rabbit AlexaFluor488 (Molecular Probes, A-21206) as secondary antibodies. For VWF detection, the following antibodies were used: (i) Immunofluorescence, monoclonal mouse anti-VWF (Dako, M0616) and anti-mouse AlexaFluor568 (Molecular Probes, A-11004) as secondary antibodies; (ii) ELISA-based secretion assay, polyclonal rabbit anti-VWF (Dako, A008202) and polyclonal rabbit anti-VWF-HRP (Dako, P0226) antibodies. Mouse monoclonal anti-S100A10 (BD Transduction Laboratories, 610071) and anti-AnxA2 antibodies (HH7) were described previously (Osborn *et al.*, 1988). Mouse monoclonal anti-penta-Histidine antibodies (Qiagen, 34660) and mouse monoclonal anti-Rab27a antibodies (Santa Cruz, sc-74586) were used to detect His_6-tagged Munc13-4 and Rab27a, respectively.

Plasmids and siRNA

The following Munc13-4 constructs were described previously: YFP-Munc13-4, GFP-Munc13-4(543-1090), GFP-Munc13-4(1-899), GFP-Munc13-4(285-917), GFP-

Munc13-4(Δ280-285) (Neeft *et al.*, 2005; Elstak *et al.*, 2011), Munc13-4-mKate, Munc13-4(C2A*)-mKate (D127N and D133N), Munc13-4(C2B*)-mKate (D941N and D947N), Munc13-4(C2A*C2B*)-mKate (D127N, D133N, D941N, and D947N) (Boswell *et al.*, 2012). YFP-Munc13-4(1-780) and YFP-Munc13-4(781-1090) were generated from YFP-Munc13-4 using the following primers: 1-780FW (5'CTACTCTCGAGCCATGGCGACACTC) and 1-780REV (5'GAAACTGGTGGGCTAGCTCGAGGAGAG; 781-1090FW (5'GAGAGCTCGA GCCGTCAGGGAGTCTG) and 781-1090REV (5'CGGCCGGCACCGTAGCTCGAGGAGAG). YFP-S100A10 (Zobiack *et al.*, 2001) and AnxA2-GFP (Rescher *et al.*, 2000) were described previously, as was the VWF-RFP plasmid (Babich *et al.*, 2008), which was kindly provided by Tom Carter (St. George University, London, UK). For the in vitro binding assays, we used the following His_6-tagged variants of Munc13-4 cloned into the bacterial expression vector pET28a via XhoI restriction sites: His_6-Munc13-4(1-1090), His_6-C2A-MUN(1-887), His_6-C2B(888-1090); His_6-MUN(285-887). The S100A10 constructs (full-length S100A10, S100A10(1-90) and S100A10(1-84)) were described previously (Kube *et al.*, 1992). To deplete cells of Munc13-4 we used the siRNA 5'ACUGAAUGGUUCCACCUGA-dTdT. For control experiments, we used unspecific siRNAs (siGenome non-targeting siRNA, Dharmacon). To deplete cells of S100A10 we used the siRNA targeting the nucleotides 84-103 (5'GGAGGACCUGAGAGUACUC-dTdT) of the human coding sequence (Kube *et al.*, 1992).

YFP-Munc13-4 and GFP-Munc13-4(Δ280-285) were rendered insensitive to the Munc13-4-specific siRNA by site-directed mutagenesis with the following mutagenesis primer (mutated nucleotides in small caps): 5'CAGACTGGCACCACcGAg-TGGTTtCAtCTcAAGCAGCAGCACC. Rab27a was depleted using the siRNA 5`GGAGAGGUUUCGUAGCUUA-dTdT (Sigma).

Reverse transcription PCR

RNA was isolated from HUVEC using the RNeasy Mini Kit (Qiagen) and reverse transcribed into cDNA (High-Capacity cDNA Reverse Transcription Kit, Applied Biosystems), and the PCR was performed with isoform-specific primers from PrimerBank (Wang and Seed, 2003; Spandidos *et al.*, 2008, 2010): Munc13-1 (PrimerBank primerID, 283837841c1; product size, 243 bp; forward primer,

5’CATGTTCGAGATTAACCGTCTGG; reverse primer 5’GGTAGCTCAAAGCGCGTGT); Munc13-2 (PrimerBank primerID, 110611225c1; product size, 159 bp; forward primer, 5’CTCTGCGTGCGCGTTAAAAG; reverse primer, 5’CAGGCGACTAATCTCAAACATGA); Munc13-3 (PrimerBank primerID, 12293 7513c2; product size, 168 bp; forward primer, 5’CCAATGGCCTACAAAAGAATGC; reverse primer, 5’TTCTGTTGCGTCTAACTGGCA); Munc13-4 (PrimerBank primerID, 120432045c1; product size, 201 bp; forward primer, 5’TCTACGAGGACGCACTCTACA; reverse primer, 5’CCTTGGCCTGTTTCACTGTTG). PCRs were carried out with KapaHifi (Kapa Biosystems) at the following conditions: 95°C for 5 min; cycle 98°C for 30 s, 55°C for 30 s, 72°C for 40 s, 35 cycles; final elongation 72°C for 5 min. PCR samples were subjected to electrophoresis on 3% agarose gels.

Surface plasmon resonance (SPR) measurements

SPR experiments were performed with a Biacore 3000 system with a M5 sensor chip (GE Healthcare). The HBS-P flow buffer [10 mM HEPES (pH 7.4), 150 mM NaCl, 0.005% (v/v) Tween 20] was filtered through 0.22 µm filters (Millipore) and degassed before use. About 800 response units (RU) of purified Munc13-4 were immobilized on the sensor chip using the amine coupling method according to the manufacturer’s instructions. Briefly, using a flow rate of 5 µm/min, the chip surface was activated with a 7 min injection of a freshly prepared 1:1 mixture of 0.2 M N-ethyl-N(3-diethylaminopropyl) carbodiimide (EDC) and 0.05 M N-hydroxysuccinimide (NHS) solution, followed by injection of Munc13-4 at a concentration of 30 µg/mL in acetate buffer, pH 5.0. As soon as the desired level of immobilization was achieved, unreacted N-hydroxysuccinimide-ester groups were blocked with a 7 min injection of 1 M ethanolamine hydrochloride. Sensograms (RU versus time) were recorded at 25°C with a typical flow rate of 30 µl/min and injection times of 3 minutes. Controls for the contribution of the change in bulk refractive index were performed in parallel with blank flow cells, which were activated with EDC/NHS and deactivated with ethanolamine in the absence of protein to be coupled, and subtracted from all binding sensograms. Blank injections of the running buffer were also performed and substracted from all kinetic measurements. To analyze the binding of S100A10 to the immobilized Munc13-4, different concentrations of S100A10 diluted in the flow buffer over a concentration range of 0.9-7.1 µM were injected into the flow cells. Each

injection was repeated at least twice to ensure reproducibility. Regeneration of the surface was performed using two short pulses of 10 mM glycine of pH 2.2. Approximate equilibrium dissociation constants (K_D) were obtained by measuring the equilibrium resonance (R_{eq}) units at several ligand concentrations at equilibrium. The affinity of the interaction was determined from the level of binding at equilibrium as a function of the sample concentrations by BIAevalution version 4.1 software (Biacore, Inc.).

References

Babich, V., Meli, A., Knipe, L., Dempster, J. E., Skehel, P., Hannah, M. J., and Carter, T. (2008). Selective release of molecules from Weibel-Palade bodies during a lingering kiss. Blood 111, 5282–5290.

Boswell, K. L., James, D. J., Esquibel, J. M., Bruinsma, S., Shirakawa, R., Horiuchi, H., and Martin, T. F. J. (2012). Munc13-4 reconstitutes calcium-dependent SNARE-mediated membrane fusion. J. Cell Biol. 197, 301–312.

Elstak, E. D. et al. (2011). The munc13-4-rab27 complex is specifically required for tethering secretory lysosomes at the plasma membrane. Blood 118, 1570–1578.

Kube, E., Becker, T., Weber, K., and Gerke, V. (1992). Protein-protein interaction studied by site-directed mutagenesis. Characterization of the annexin II-binding site on p11, a member of the S100 protein family. J. Biol. Chem. 267, 14175–14182.

Man, K. N. M., Imig, C., Walter, A. M., Pinheiro, P. S., Stevens, D. R., Rettig, J., Sørensen, J. B., Cooper, B. H., Brose, N., and Wojcik, S. M. (2015). Identification of a Munc13-sensitive step in chromaffin cell large dense-core vesicle exocytosis. eLife 4.

Neeft, M. et al. (2005). Munc13-4 is an effector of rab27a and controls secretion of lysosomes in hematopoietic cells. Mol. Biol. Cell 16, 731–741.

Osborn, M., Johnsson, N., Wehland, J., and Weber, K. (1988). The submembranous location of p11 and its interaction with the p36 substrate of pp60 src kinase in situ. Exp. Cell Res. 175, 81–96.

Rescher, U., Zobiack, N., and Gerke, V. (2000). Intact Ca(2+)-binding sites are required for targeting of annexin 1 to endosomal membranes in living HeLa cells. J. Cell Sci. 113, 3931–3938.

Shirakawa, R., Higashi, T., Tabuchi, A., Yoshioka, A., Nishioka, H., Fukuda, M., Kita, T., and Horiuchi, H. (2004). Munc13-4 Is a GTP-Rab27-binding Protein Regulating Dense Core Granule Secretion in Platelets. J. Biol. Chem. 279, 10730–10737.

Spandidos, A., Wang, X., Wang, H., Dragnev, S., Thurber, T., and Seed, B. (2008). A comprehensive collection of experimentally validated primers for Polymerase Chain Reaction quantitation of murine transcript abundance. BMC Genomics 9, 633.

Spandidos, A., Wang, X., Wang, H., and Seed, B. (2010). PrimerBank: a resource of human and mouse PCR primer pairs for gene expression detection and quantification. Nucleic Acids Res. 38, D792–D799.

Varoqueaux, F., Sons, M. S., Plomp, J. J., and Brose, N. (2005). Aberrant Morphology and Residual Transmitter Release at the Munc13-Deficient Mouse Neuromuscular Synapse. Mol. Cell. Biol. 25, 5973–5984.

Wang, X., and Seed, B. (2003). A PCR primer bank for quantitative gene expression analysis. Nucleic Acids Res. 31, e154–e154.

Zobiack, N., Gerke, V., and Rescher, U. (2001). Complex formation and submembranous localization of annexin 2 and S100A10 in live HepG2 cells. FEBS Lett. 500, 137–140.

Supplementary figures

Figure S1. Depletion of Rab27a.

a) Western blot detection of Rab27a in lysates of HUVEC transfected for 48 h with a Rab27a-specific siRNA or unspecific siControl using mouse monoclonal anti-Rab27a antibodies. Vimentin served as loading control.

b) Quantification of the fraction of Munc13-4 colocalizing with WPBs. The association of Munc13-4 with WPBs was quantified in HUVEC transfected for 48 h with YFP-Munc13-4 and either unspecific siControl (sControl) or Rab27a-specific siRNA (siRab27a), or with only GFP-Munc13-4 (Δ280-285) (Δ280-285). WPBs were visualized by labeling with anti-VWF antibodies and colocalization analysis was carried out as described in Materials and methods. Mean colocalizations on WPBs from at least 10 cells per condition of at least three independent experiments were tested for statistical significance by one-way ANOVA with Tukey's test (ns, not statistically significant). Total numbers of WPBs, n, were as follows: siCtrl, n=732; siRab27a, n=437; Δ280-285, n=572. Bars represent mean±SEM.

Figure S2. Quantification of WPB localization of different Munc13-4 mutants

The association of Munc13-4 with WPBs was quantified in HUVEC transfected for 24 h with either full-length YFP-Munc13-4, YFP-Munc13-4(543-1090), GFP-Munc13-4(1-899), GFP-Munc13-4(285-917), YFP-Munc13-4(781-1090), or YFP-Munc13-4(1-780). WPBs were visualized by labeling with anti-VWF antibodies and colocalization analysis was carried out as described in Materials and methods. Mean colocalizations on WPBs from at least 10 cells per condition of at least three independent experiments were tested for statistical significance by one-way ANOVA with Tukey's test (ns, not statistically significant, **** $p \leq 0.0001$ as compared to full-length YFP-Munc13-4). Total numbers of WPBs, n, were as follows: Munc13-4, n=523; Munc13-4(543-1090), n=402; Munc13-4(1-899), n=511; Munc13-4(285-917), n=399; Munc13-4(781-1090), n=322; Munc13-4(1-780), n=177. Bars represent mean±SEM.

Figure S3. Quantification of total VWF levels after Munc13-4 knockdown

Comparison of the levels of total VWF in the Munc13-4 knockdown experiments shown in figure 4b. Total VWF is the sum of VWF in the supernatant of non-stimulated cells, the supernatant of stimulated cells and the remaining total lysate (for

details see to Materials and methods). Shown are means of at least five independent experiments that were tested for statistical significance by one-way ANOVA with Tukey's test (ns, not statistically significant). Bars represent mean±SEM. The numbers of independent experiments n were as follows: siControl + YFP or Munc13-4, n=8; siControl + Δ280-285, n=7; siMunc13-4 + YFP or Munc13-4, n=6; siMunc13-4 + Δ280-285, n=5.

Figure S4. Forskolin stimulation does not trigger the formation of Munc13-4 foci at sites of WPB exocytosis.

(a) TIRF sections of live HUVEC expressing YFP-Munc13-4 and VWF-RFP as WPB marker and stimulated with 40 μM forskolin and 100 μM IBMX at t=0 s. Arrowheads indicate fusing WPBs. Scale bar represents 10 μm.

(b) Representative graph showing the number of Munc13-4-positive objects detected in the TIRF field of the HUVEC shown in (a) expressing YFP-Munc13-4 and VWF-RFP, stimulated with 40 μM forskolin and 100 μM IBMX at t=20 s.

(c) Change in the number of Munc13-4-positive objects per 100 μm^2 after stimulation with 100 mM histamine or 40 μM forskolin and 100 μM IBMX. Means of n-fold changes over all cells from at least three independent experiments were tested for statistical significance by unpaired t-test (**** p≤0.0001). Numbers of cells analyzed, n, were as follows: Munc13-4 (histamine), n=32; Munc13-4 (forskolin), n=13. Means±SEM: 2.8±0.1/1.3±0.06.

Note that forskolin stimulation triggers WPB fusion (a), but no formation of Munc13-4 foci (b, c).

Figure S5. Interaction of Munc13-4 with S100A10 analyzed by surface plasmon resonance.

(a) Eight-hundred response units (RU) of purified Munc13-4 were immobilized on the CM5 sensor chip using the amine coupling method. S100A10 at concentrations ranging from 0.9 to 7.1 μM was injected and allowed to react with the sensor chip surface at a flow rate of 30 μl/min and an injection time of 3 min. The average binding level at the end of injection (equilibrium) was used for calculation of the steady-state affinity K_D.

(b) Steady state affinity determined from the level of binding at equilibrium (R_{eq}) as a function of the sample concentration.

Figure S6. Histamine stimulation triggers a recruitment of S100A10 and AnxA2 to the plasma membrane.

HUVEC expressing YFP-S100A10 (**a**) or AnxA2-GFP (**b**) were subjected to histamine stimulation and analyzed by live-cell TIRF microscopy. Shown are representative stills of the respective videos depicting a cell before and after stimulation. Note that S100A10 and AnxA2 show a general recruitment to the plasma membrane following histamine stimulation. See also supplementary videos FigS6video03 and FigS6video04.

(c) Partial colocalization of S100A10 with stimulation-induced Munc13-4 foci. HUVEC expressing Munc13-4-mKate and YFP-S100A10 were stimulated with histamine and subjected to live cell confocal microscopy recordings. Shown are stills of a representative time-lapse movie, where cells were stimulated with histamine at t=0 s. Arrowheads indicate the enrichment of S100A10 at Munc13-4 foci that occur at WPB fusion sites. See also supplemental video FigS6video05.

Scale bars represent 10 µm (a, b) and 5 µm (c).

Figure S7. Depletion of Munc13-4 and S100A10 in single and double knockdown experiment.

Western blot detection of HUVEC lysates treated with an unspecific siRNA as control (siControl), or depleted of either Munc13-4 or S100A10 individually or of Munc13-4 and S100A10 in a double knockdown experiment. Blots were probed with anti-Munc13-4, anti-S100A10 antibodies and anti-calnexin antibody as loading control.

Supplementary videos

Fig5video01. TIRF time-lapse recording of a WPB positive for YFP-Munc13-4 (left panel; green in the merge panel on the right) and VWF-RFP (middle panel; red in the merge panel on the right). HUVEC were stimulated with 100 µM histamine at t=0 s. Frames were taken twice per second, display rate is five frames per second. Scale bar represents 1 µm. Stills from this recording are shown in figure 5b.

Fig6video02. TIRF time-lapse recording of a cell expressing YFP-Munc13-4 (left panel; green in the merge panel on the right) and VWF-RFP (middle panel; red in the merge panel on the right). HUVEC were stimulated with 100 µM histamine at t=0 s. Frames were taken twice per second, display rate is 21 frames per second. Scale bar represents 10 µm. Stills from this recording are shown in figure 6a.

FigS6video03. TIRF time-lapse recording of a cell expressing YFP-S100A10. HUVEC were stimulated with 100 µM histamine at t=0 s. Frames were taken twice per second, display rate is seven frames per second. Scale bar represents 10 µm. Stills from this recording are shown in figure S6a.

FigS6video04. TIRF time-lapse recording of a cell expressing AnxA2-GFP. HUVEC were stimulated with 100 µM histamine at t=0 s. Frames were taken twice per second, display rate is seven frames per second. Scale bar represents 10 µm. Stills from this recording are shown in figure S6b.

FigS6video05. Confocal time-lapse recording of a cell expressing S100A10-YFP and Munc13-4-mKate. HUVEC were stimulated with 100 µM histamine at t=0 s. Frames were taken every 2.8 seconds, display rate is seven frames per second. Scale bar represents 5 µm. Stills from this recording are shown in figure S6c.

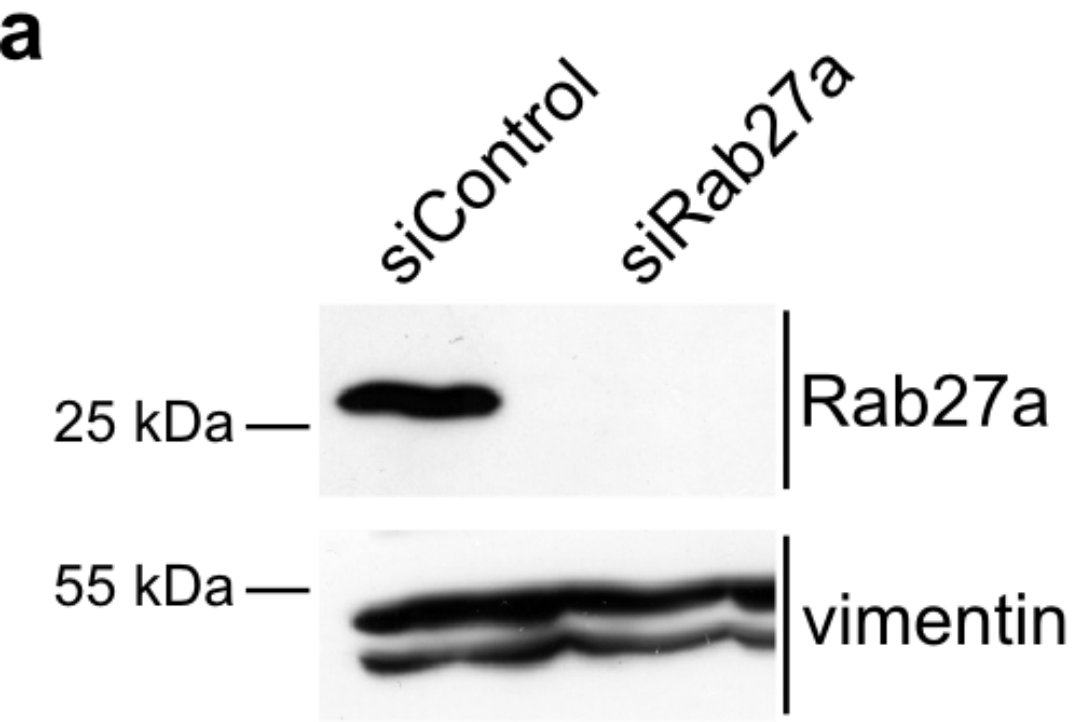
a
siControl
siRab27a
25 kDa
Rab27a
55 kDa
vimentin

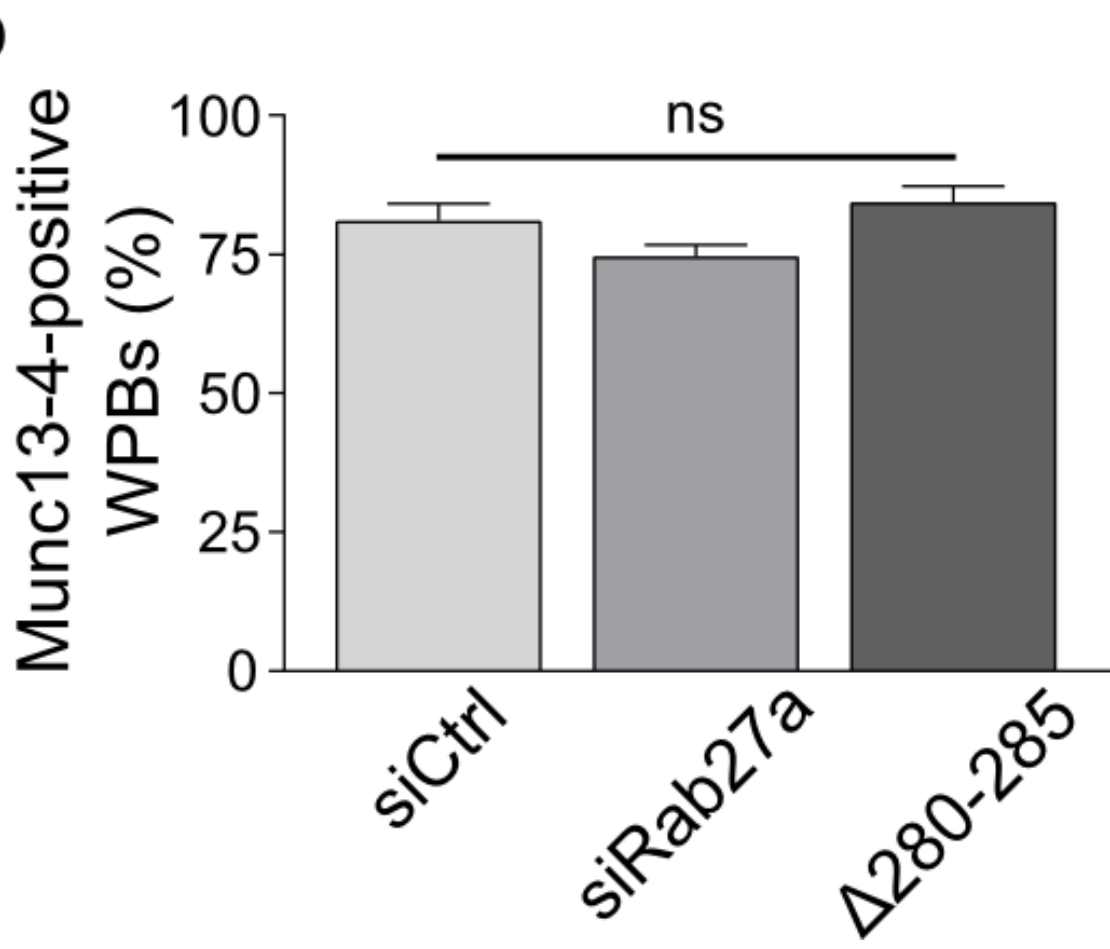
b
Munc13-4-positive WPBs (%)
100
75
50
25
0
ns
siCtrl
siRab27a
Δ280-285

Fig.S1

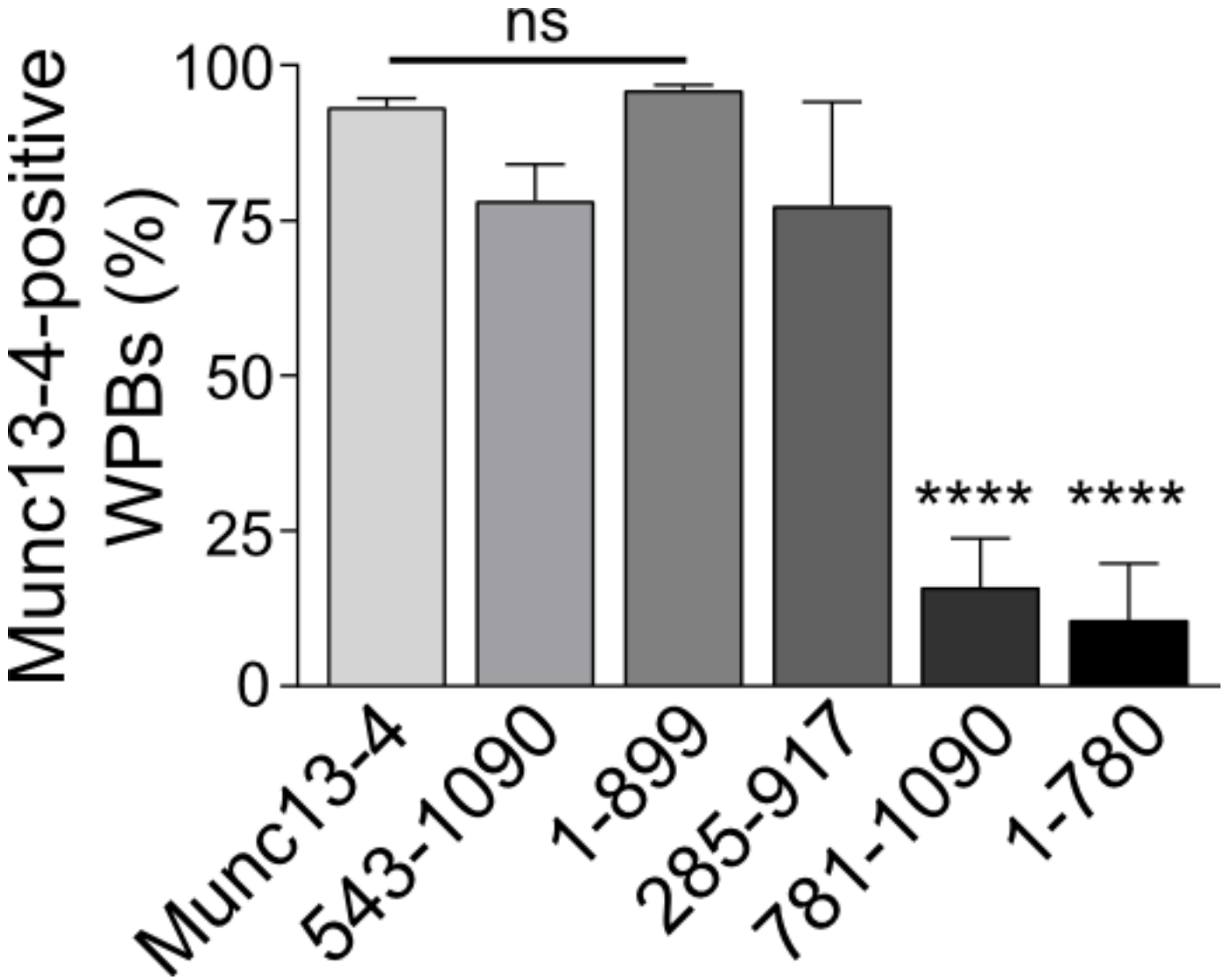
ns
100
75
50
25
0
Munc13-4-positive WPBs (%)
****
****
Munc13-4
543-1090
1-899
285-917
781-1090
1-780

Fig.S2

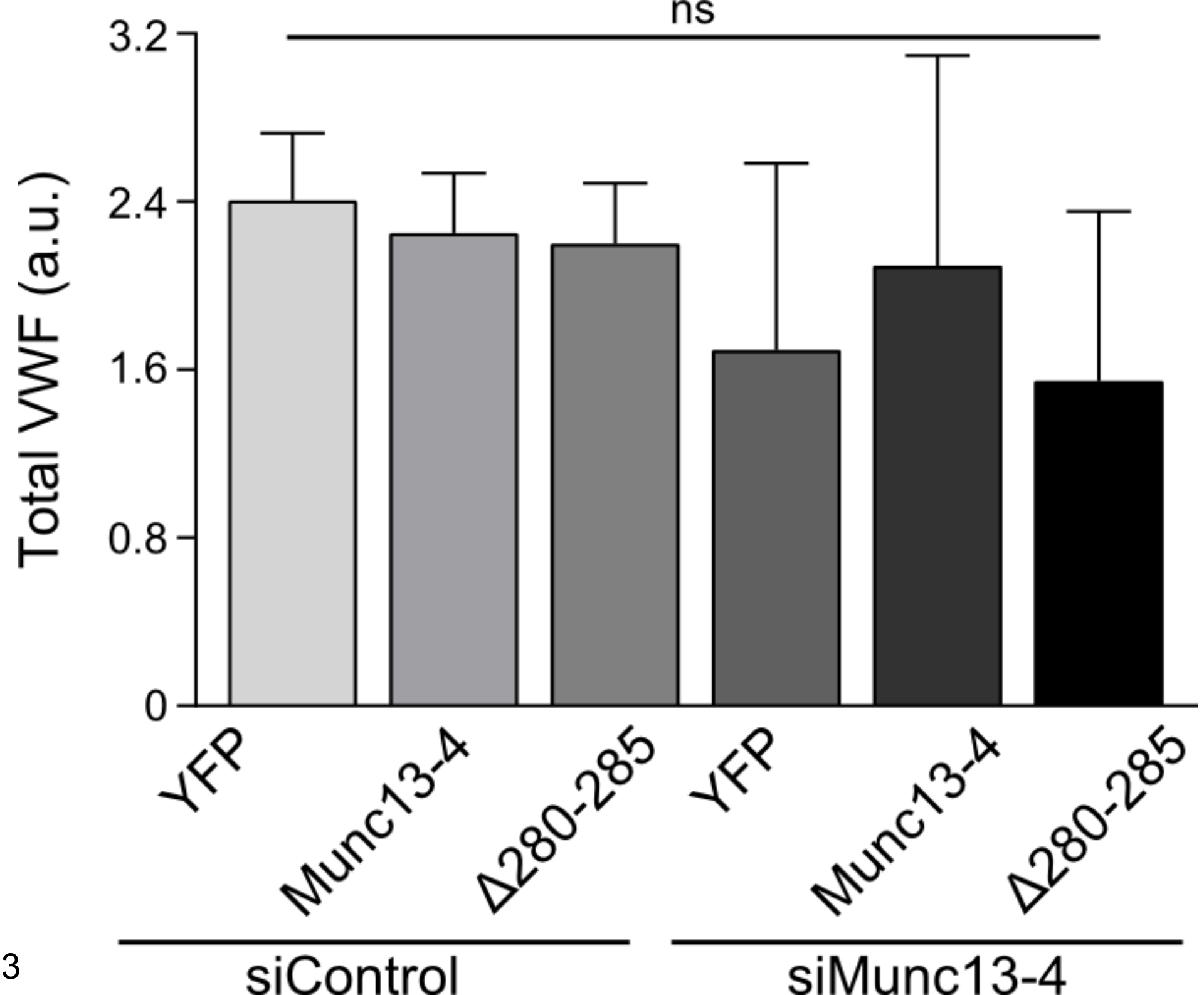
ns
3.2
2.4
1.6
0.8
0
Total VWF (a.u.)
YFP
Munc13-4
Δ280-285
YFP
Munc13-4
Δ280-285
siControl
siMunc13-4

Fig.S3

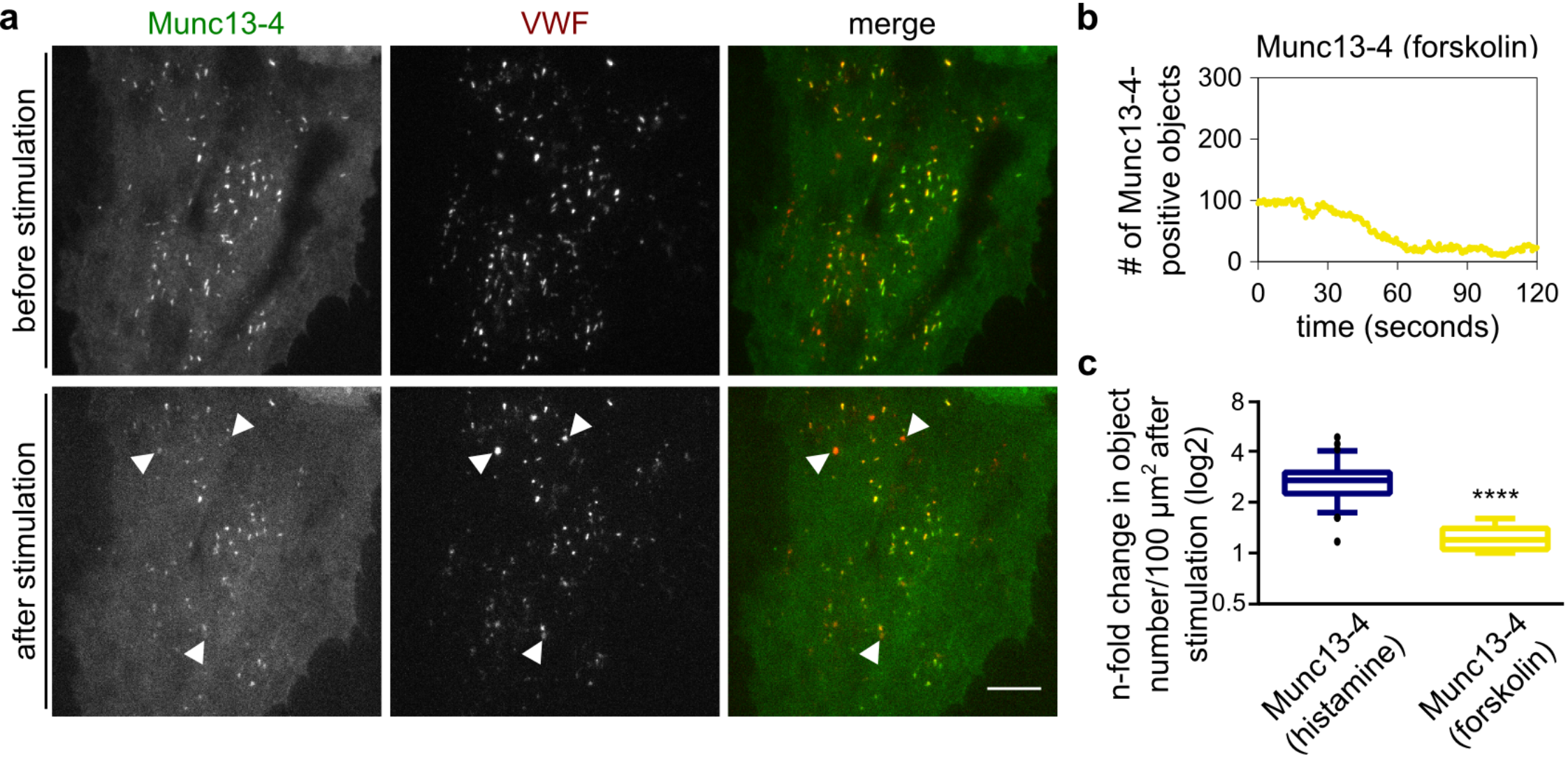
a
Munc13-4
VWF
merge
before stimulation
after stimulation
b
Munc13-4 (forskolin)
# of Munc13-4-positive objects
300
200
100
0
0
30
60
90
120
time (seconds)
c
n-fold change in object number/100 µm² after stimulation (log2)
8
4
2
1
0.5
****
Munc13-4 (histamine)
Munc13-4 (forskolin)

Fig.S4

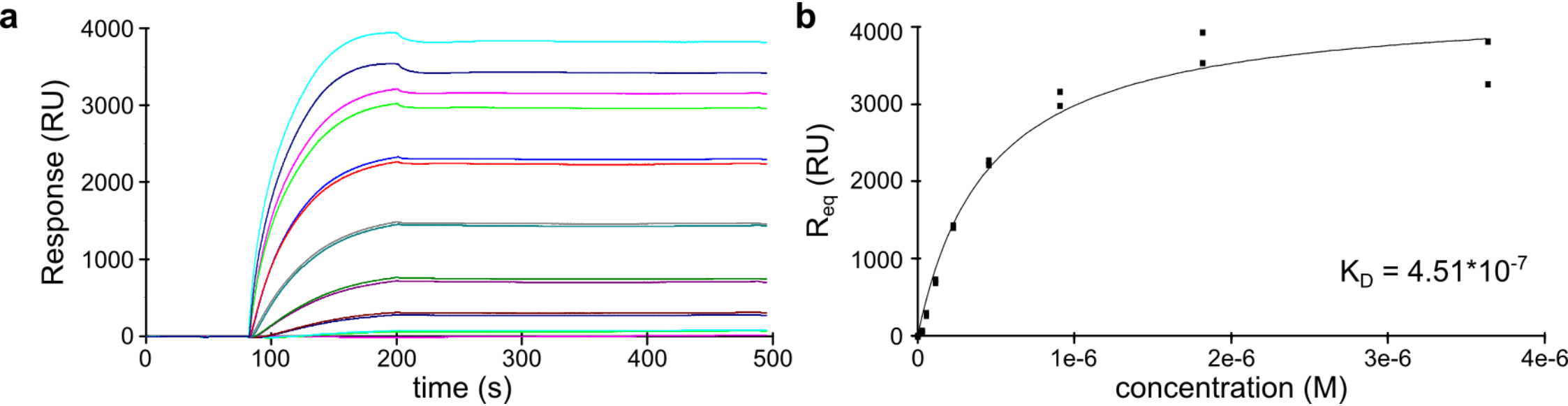
a
Response (RU)
4000
3000
2000
1000
0
0
100
200
300
400
500
time (s)
b
R_{eq} (RU)
4000
3000
2000
1000
0
0
1e-6
2e-6
3e-6
4e-6
concentration (M)
$K_D = 4.51*10^{-7}$

Fig.S5

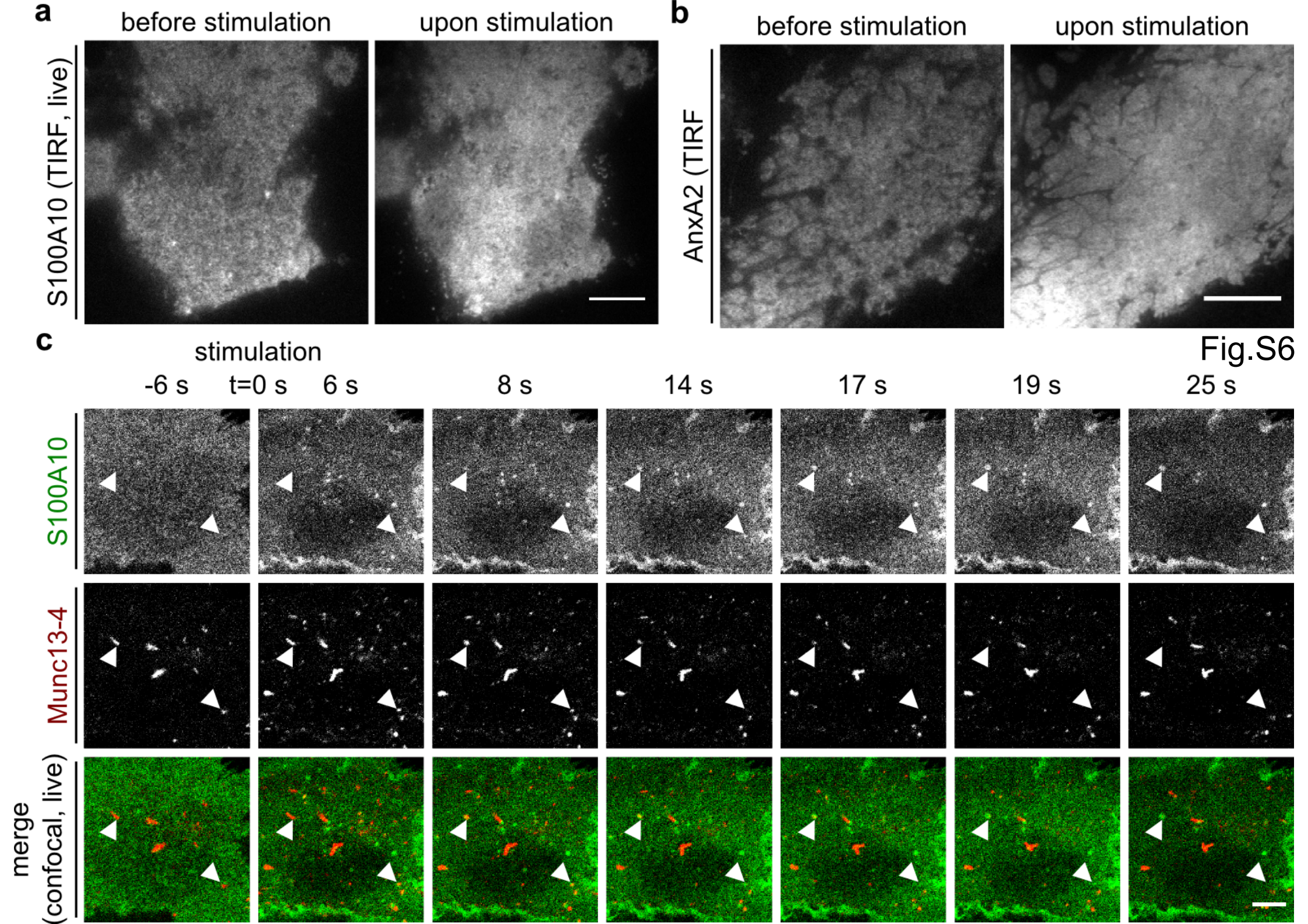
a
before stimulation
upon stimulation
S100A10 (TIRF, live)
b
before stimulation
upon stimulation
AnxA2 (TIRF
c
stimulation
-6 s
t=0 s
6 s
8 s
14 s
17 s
19 s
25 s
S100A10
Munc13-4
merge
(confocal, live)

Fig.S6

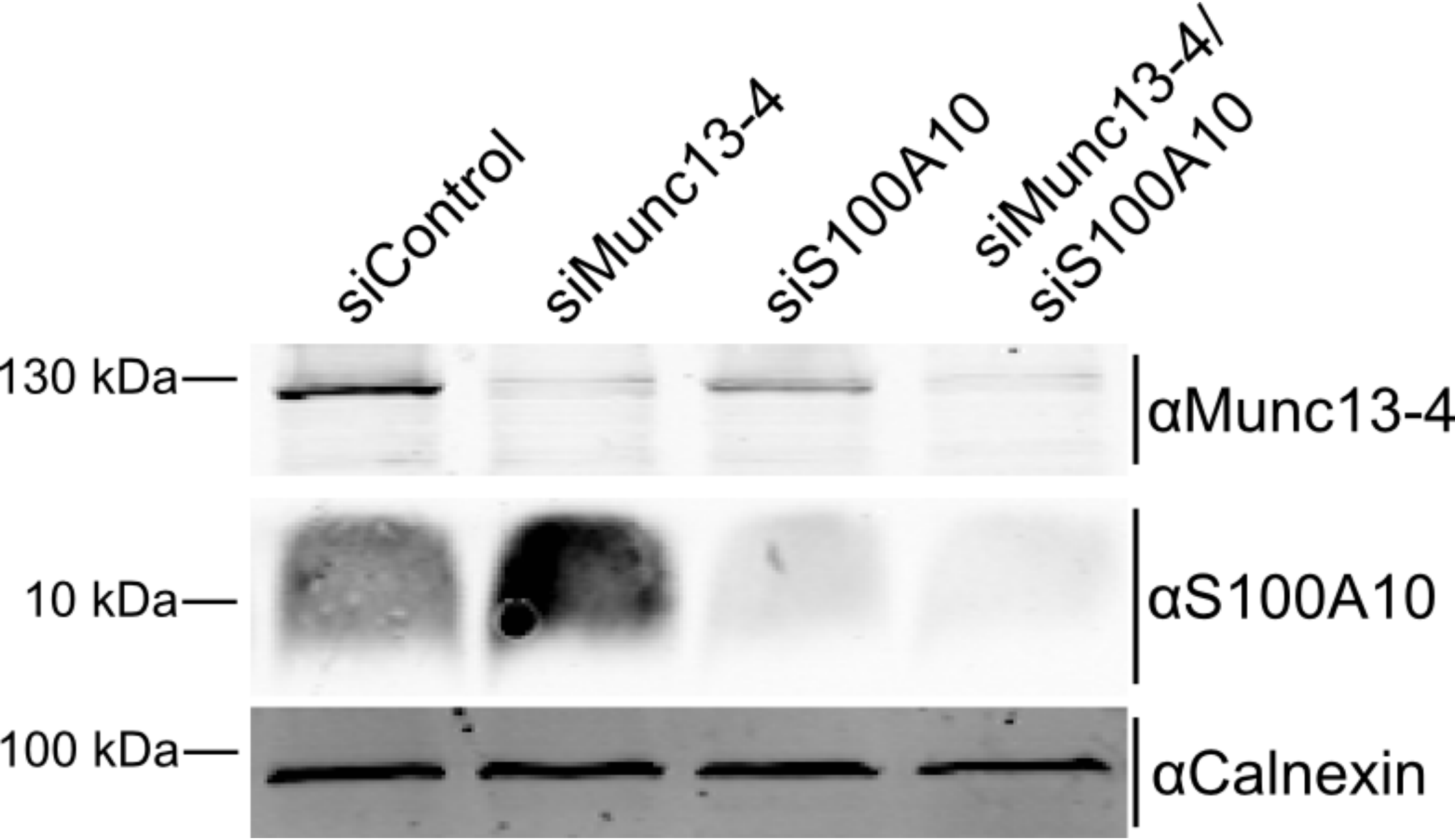
siControl
siMunc13-4
siS100A10
siMunc13-4/
siS100A10
130 kDa—
αMunc13-4
10 kDa—
αS100A10
100 kDa—
αCalnexin

Fig.S7